GLOBAL HEALTH SECURITY AND DISASTER FORENSICS: A SOLUTION ORIENTED APPROACH TO MAPPING PUBLIC HEALTH VULNERABILITIES THROUGH PREDICTIVE ANALYTICS

NATHANAEL STANLEY; BENJAMIN G. JACOB; ANTHONY J MASYS; JEEGAN PARIKH; RICARDO IZURIETA; MIGUEL REINA

College of Public Health, University of South Florida, USA
e-mail tmasys@health.usf.edu

ABSTRACT

Heyman et al., (2015:1888) argues that, "the world is ill-prepared" to handle any "sustained and threatening public-health emergency". Such public health emergencies stemming from infectious disease outbreaks is creating a serious threat to global health security. For example, climate change and extreme weather events threaten to alter and affect geographic areas pertaining to disease vulnerability, such as greater risks of mosquito-borne diseases (dengue, malaria, yellow fever and Zika). The emergence of these disease outbreaks and their influence globally has sparked a renewed attention on global health security. In the Chatham House report 'Preparing for High Impact, Low Probability Events', Lee et al (2012:vii) '…found that governments and businesses remain unprepared for such events'. Recent outbreaks characterize the 'new normal' and has unveiled major deficiencies in preparedness, response and recovery initiatives. For example, Ae. aegypti is one of the most significant mosquito species as it is capable of transmitting dengue fever, chikungunya, Zika, and yellow fever viruses. Understanding the emerging threat employing landscape real time epidemiological tools may 'experimental futuring' and scenario planning, this paper presents novel methods to predictively understand the processes by which species colonize and adapt to human habitats with a focus on the case of a virulent disease-vectoring arthropod such as Ae. aegypti. In this paper, we introduce real time ArcGIS machine learning (ML), spectral signatures in unmanned semi-Autonomous drone aircraft platform for controlling Ae. aegypti. mosquito habitats. The multivariate real time platform regressed the spatial risk of human exposure to Ae. aegypti pathogens to forecast unknown capture point georeferenceable geolocations of elevated risk. In so doing, the methodology described strengthens mitigation, preparedness, response and recovery through vulnerability analysis and predictive analytics.

Keywords: experimental futures analysis; scenario planning; GIS; predictive analytics; disaster forensics

1   INTRODUCTION

Heyman et al., (2015:1888) argues that, "the world is ill-prepared" to handle any "sustained and threatening public-health emergency". Such public health emergencies stemming from infectious disease outbreaks is creating a serious threat to global health security. The complex spatial-temporal dynamics associated with climate related events, social, economic, political and environmental problem space influence the emergence and distribution of vector-borne diseases (VBDs) thereby shaping the public health landscape. Similarly, natural disasters such as earthquakes, landslide and flooding are not only physically destructive to communities but also are precursors to public health disasters. For example, as discussed in Reina Ortiz et al., (2017:1) 'Natural disasters, like earthquakes, are often associated with or followed by serious public health consequences such as increased risk for communicable diseases, including waterborne and vector-borne diseases'. This emerges from the impact of disasters on creating conditions that are conducive to mosquito breeding.

Climate change and the increase in the severity of natural disasters has compromised public health conditions particularly in vulnerable communities thereby highlighting disparities across populations defined spatially. As noted by Bardosh et al., (2017:6), '…VBDs are also influenced by the context of social, cultural and political change, which have major effects on the social determinants of health, mediating financial flows and human resources and shaping the delivery of healthcare services and disease prevention initiatives'. The World Health Organization (WHO) argue that Climate change has been identified as "the defining issue" for public health in the 21st century' (Sheehan,Fox, Kaye,& Resnick, 2017). The disease aetiology connecting VBDs and climate change emerges from the effect on life cycle of disease vectors and transmission potential of pathogens

(Berrang-Ford et al., 2016). Bardosh et al., (2017) argue that '…The threat of a rapidly changing planet – of coupled social, environmental and climatic change – pose new conceptual and practical challenges in responding to vector-borne diseases. These include non-linear and uncertain spatial-temporal change dynamics associated with climate, animals, land, water, food, settlement, conflict, ecology and human socio-cultural, economic and political-institutional systems'. Recognizing the complex interdependencies provides insights into disaster scenario development and ensuing mitigation and preparedness awareness.

As described in Reina Ortiz et al (2017) '…anthropogenic climate change has led to changing global temperatures, which may be associated with changes in rainfall as well as other important climatic variables like humidity and pressure'. Such changes have significant public health implications, particularly as is relates to optimizing conditions to support vector-borne disease superbreeder sites. This coupled with natural disasters creates conditions for the 'perfect storm' that can lead to an increase in the public health burden of vector-borne diseases. Reina Ortiz (2017) argue that

'Climatic variables are known to affect vector-borne diseases transmission. The rise in vector-borne diseases such as dengue and malaria has been found to have a direct relationship with the occurrence of strong El Niño events. Similarly, vector-borne diseases have been found to be associated with Surface Sea Temperatures and the Tropical South Atlantic'.

In addition to the biophysical aspects of the problem space are the social dimensions associated with VBD and climate related disasters. Bardosh et al (2017:7) argue that 'Poverty enhances vulnerability to VBDs in multiple ways, mainly by removing the capacity for people to cope with and address health risks. Different temporal and spatial scales are at play, and extend across a diverse number of social, cultural, political, economic, environmental, climatic, and biological determinants'. The hazard of place model (Cutter, 1996), figure 1, captures the climate change and extreme weather impact geospatial/temporal and social dimensions discussed. By recognizing the geospatial/temporal and social dimensions of a climate change induced disaster, we highlight the application of predictive analytics to support scenario planning and mitigation strategy development. Bardosh et al. (2017:16) highlight the urgency for action:

'The importance of resilient global health systems to deal with vector-borne infections, and indeed most other human health threats, is truly a matter of life and death. There is little doubt that the spectrum of social, environmental and climatic changes occurring simultaneously in the twenty-first century will impact the distribution and incidence of VBD's'.

Within the context of climate related events and the Hazard of Place model, 'the rise in vector-borne diseases such as dengue and malaria has been found to have a direct relationship with the occurrence of strong El Niño events' (Reina Ortiz et al., 2017) as well as in the Tropical South Atlantic stemming from perturbations in Surface Sea Temperatures. Hence, through experimental futuring supported by predictive analytics we can better develop place vulnerability awareness (biophysical, social, spatial).
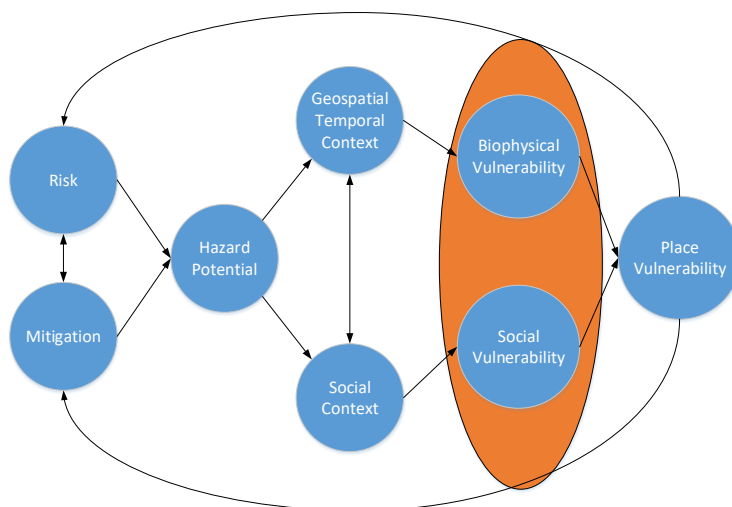

Figure 1. Hazard of Place model (Cutter, 1996)

2   DISCUSSION

The hazard place model (Cutter, 1996) captures well the complex interactions between the biophysical stressors and social vulnerabilities within a geospatial context. This presents an opportunity for the design of scenario planning and mitigation strategy development by exploring the vulnerabilities associated with place. In support of this, real-time predictive analytic solutions were developed.

We develop a customized, iOS application (app) for identifying geographic locations (henceforth geolocations) of superbreeder, *Aedes aegypti,*, capture point, habitat properties in Hillsborough County, Florida, USA from real time acquisitions of sub-meter resolution (e.g., 30 centimeter), land use land cover (LULC) , ecologically georeferenced (henceforth eco-georeferenced), images obtained from a drone unmanned aircraft. Initially we created experimental, *Ae. aegypti,* breeding sites in a variety of differentially stratified, LULC classifications (e.g., recreational parklands, agro-industrial pasturelands and urban residential   settings). Wayward, differentially corrected, GPS proposed, custom flight plans were then overlaid onto ArcGIS models of the classified land covers throughout Hillsborough County so that local mosquito control personnel and USF research collaborators were able to create collections of the habitat imagery at the county-level. The images were analyzed to optimally identify unbiased, capture point, Red Green and Blue (RGB), wavelength signatures unique to the artificial breeding sites. We collected images from the experimental sites using a drone (DJ Phantom) carrying a camera capable of producing wide-angle high-resolution images (Figure 2).

Figure 2. A high-end radio-controlled Phantom 2 Vision+ camera-equipped quadcopter

Spectral signature of a vector arthropod, aquatic, larval/pupal habitat is the variation of reflectance or emittance of breeding site material (e.g., canopied, capture point, eco-georeferenced, LULC, seasonal foci) with respect to wavelengths (i.e., reflectance/emittance as a function of RGB wavelengths)(Jacob et al. 2013, Jacob et al. 2011). The spectral signature of an object is a function of the incidental, electromagnetic, wavelength and material interaction with that section of the electromagnetic spectrum(Jensen 2005). The signal measurements can be with various, real time, UAV instruments, including a task specific spectrometer, which can conduct multiple, unmixing, algorithmic, real time tasks in ArcGIS [e.g. separation of a capture point, RGB and near infrared NIR) surface reflux proportions as acquired by digital cameras]. Calibrating, sub-meter resolution, RGB, spectral, *Ae aegypti* ,capture point, LULC, reflux signatures under specific illumination allowed applying an empirical correction to the real time UAV imager employing DroneDeploy 3D Map software (www.esri.com). Our assumption was that the unmixed interpolative, RGB, sub-pixel (i.e., endmember) weights could reveal unsampled, productive seasonal foci based on eco-georeferenced, LULC, geolocations of known super breeder, capture point foci. In the mathematical field of numerical analysis, interpolation is a method of constructing new data points within the range of a discrete set of known data points (Cressie 1993).

To construct a real time, UAV, *Ae aegypti*, forecast, vulnerability model for targeting unknown foci, individual pixel, 0.31, spatial resolution, geoclassified, reflectance estimates were synthesized from, experimental, eco-georeferenced, LULC, capture point, aquatic, larval/pupal habitat, epi-entomological foci employing a Li-Strahler geometric-optical model, This procedure allowed for the creation of an RGB spectral signature of a unit of habitat.   The drone model employed three LULC scene components: sunlit canopy (C), sunlit background (G) and shadow (T) generated from the real time ortho-images, to determine the. Endmember (sub-pixel) sub-meter resolution RGB spectra associated with the experimental, *Ae. aegypti*, larval/pupal, aquatic, habitat, artificial, water container, capture points (e.g., flower pot, waste tire, coffee mug etc.). The C, G and T component LULC classes were estimated using ENVI software package (Exelis Visual Information Solutions, Boulder, CO) in the UAV, real time, dashboard which employed object-based classifiers [e.g., Spectral Angle Mapper (SAM)] to delineate the capture point, RGB, spectral reflux frequencies (see Figure 3).
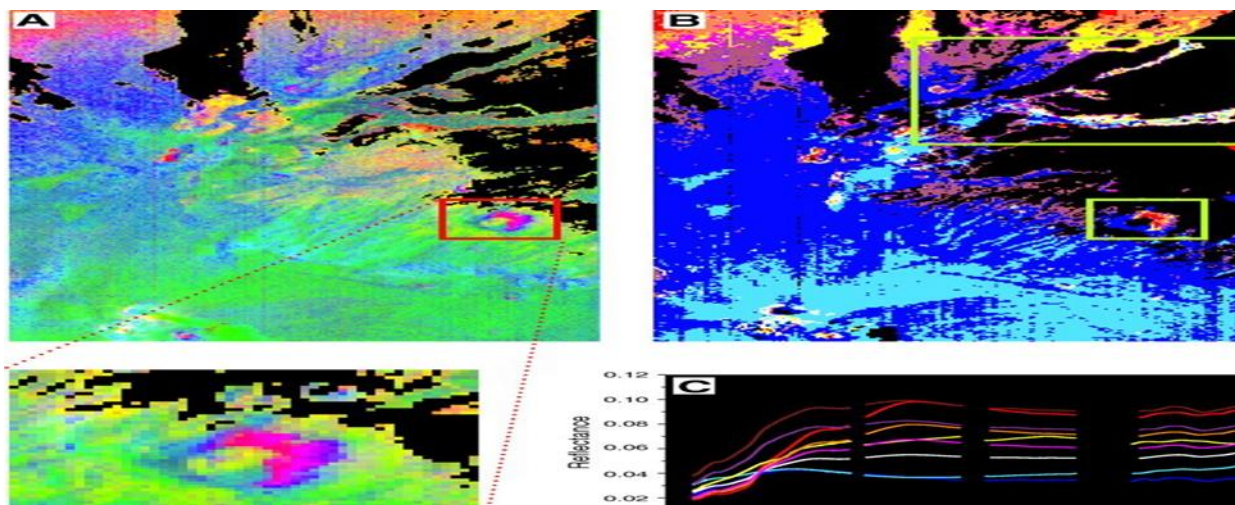
Figure 3 A) Reference signatures derived from a drone ENVI spectral library of an experimental *Ae. aegypti,* seasonal, backyard, water stagnant, flower pot foci from real-time UAV video footage B) SAM scatter matrix C) unmixed target RGB LULC signature, endemic, foci, visible and near infra-red wavelengths

SAM is a physically-based spectral classification that uses an n-D angle to match pixels to derivative, RGB reference spectra (https://www.harrisgeospatial.com/docs). Here the unmixing algorithm determined the spectral similarity between the drone imaged capture point, gridded, LULC *Ae. aegypti,* signature RGB spectra by calculating the angle between the spectra and treating them as vectors in real time geographic space (henceforth geospace). This remotely sensed technique, calibrated the reflectance, vector arthropod, while simultaneously quantitating LULC dimensionality of, the capture points which we noted as equivalent to the number of wavebands in the real time UAV environment. The technique was relatively insensitive to illumination and albedo effects. The endmember, LULC, capture point spectra employed by SAM came from the drone spectral library. We extracted them directly from orthomosaicked, , LULC images as eco-georeferenced, capture point, RGB spectra. SAM compared the angle between the endmember, RGB spectrum vector and each, capture point, habitat, pixel vector in n-D in geospace which was displayed in the real time UAV module. Smaller angles represented closer matches to the *Ae aegypti* reference signature spectrum. Capture point drone pixels in geospace further away than the specified maximum angle threshold in radians were classified in the real time UAV database as "cold spots' (noisy outliers).

Base maps were created from the UAV sampled, eco-georeferenced, seasonal, breeding site, capture point, GPS, ground coordinates using the, real time, dashboard imagery in ArcGIS. Each eco-georeferenced, *Ae. aegypti,* aquatic, larval/pupal habitat, with its associated land cover attributes, were entered into a UAV spectral library. The real time, ArcGIS dashboard module in the drone dashboard was employed to support the mobile field data acquisition, of the capture points through handheld personal digital assistants (e.g., i-tablet). All two-way, remote synchronization of data, geocoding, and spatial display was processed employing the embedded, ArcGIS Interface Kit™ geoprocessing tools in the UAV real time dashboard.

We attempted to understand potential limitations of real time, RGB, sub-meter resolution, signature,UAV interpolation to determine unknown eco-georeferenced, geolocations of *Ae aegypti* , artificial, water stagnant, ,container breeding site foci. Mosquito county abatement personnel in Hillsborough county and USF collaborators identified a number of breeding container sentinel sites and recorded their GPS locations. Habitats of varying mosquito species that were geographically located on various land cover as well as possible elevated obstructions, such as intermittently, seasonally, shade-canopied hilltops throughout Hillsborough County were identified using a 3-D digital elevation model (Figure 4a).This model was built in Geospatial 3-D Analyst in the embedded ArcGIS in the drone dashboard To determine the accuracy of the signature foci indicated by the dashboard of the LULC,eco-georeferenced, capture points, the USF team flew the drone over the test site to recover the foci to evaluate the sensitivity and specificity of the captured, real time, signatures. Drone flight plan maps for urban LULC (Figure 4b) and rural LULC (4c) were generated based on differentially corrected wayward GPS coordinates(with a positional accuracy of 0.178m) to make sure that the drone was flown over

the county abatement study site areas with precision and accuracy. The data was live streamed to ground stations, where personnel viewed the live footage using a multi-directional, mobile, hand held device (e.g., Android technology, iphone). Mosquito abatement personnel in Hillsborough County and USF researcher collaborators measured the real time, UAV captured, breeding site, capture point, ArcGIS, spectral signatures (i.e.,known habitat targets) at 31 centimeter spatial resolution.
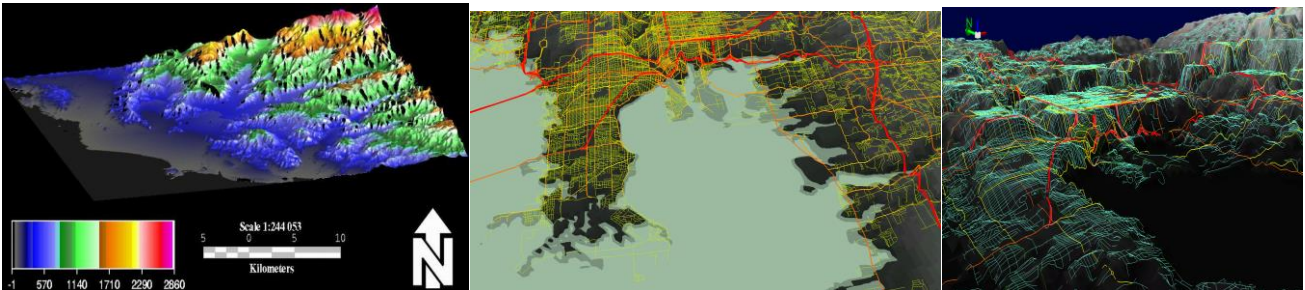
Figure 4a. A 3-D DEM   Figure 4b a drone wayward flight map of an urban location   and   Figure 4c over a rural location in Hillsborough County

We performed a log transformation using the geo- spectrally decomposed 0.31, meter resolution, real time imaged, habitat endmember, geosampled, capture point, LULC and RGB signature datasets generated in ArcGIS. For example, for an eco-georeferenced, birdbath, capture point, backyard, *Ae. aegypti*, water stagnant, artificial, container habitat in an urban residential geoclassified geolocation, the UAV model revealed that the surface reflux included the waveband ratio of 13% red, 61 % blue and 26% green (see Figure 5).
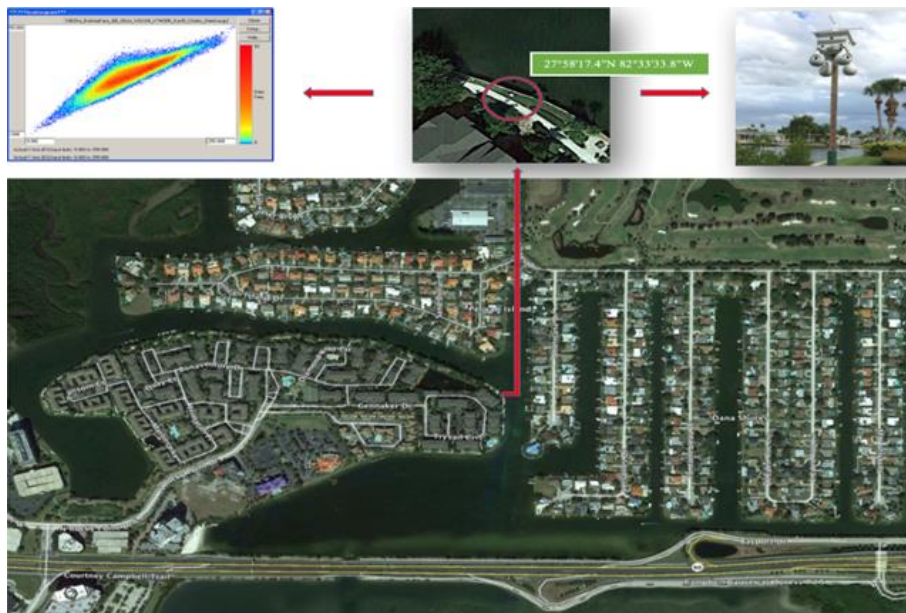
Figure 5*: Ae. aegpyti* aquatic larval/pupal habitat superbreeder backyard signature with the capture point GPS coordinate acquired from a UAV real time environment

All RGB, capture point, signature data was reviewed and contrasted in the real time platform for determining RGB wavelength, surface reflux, LULC properties for precision forecast mapping unknown, *Ae. aegypti,* larval/pupal, aquatic habitats in Hillsborough County. We optimized the UAV, spectral, signature library components from the UAV real time imaged, capture points which included object-based classifiers and a 3-D machine learning (ML) algorithm embedded in the real ArcGIS platform

Machine learning (ML) is the <u>scientific study</u> of <u>algorithms</u> and <u>statistical models</u> that <u>computer systems</u> use to effectively perform a specific task without using explicit instructions, relying on patterns and inference instead. It is seen as a subset of <u>artificial intelligence</u>.(Bishop 2006), An ML algorithm [Random Forest(RF)] was applied to our real time, geosampled, UAV, *Ae. aegypti,*,gridded, LULC datasets in ArcGIS which included the spectral signatures and priori information extracted from the capture point known locations. RF is a mixture of tree predictors that are randomly constructed by bootstrapping from the complete dataset with replacement but having the same distribution as the full dataset. Random forests of 1000 trees were trained using the VECMAP software (http://www.vecmap.com) in the real time dashboard. Six capture point, *Ae. aegypti* habitat, predictors were randomly selected at each node. Given that the input, capture point, eco-georeferenced, LULC datasets were balanced, the cut-off value to differentiate between suitable and unsuitable habitats was 0.5.

The ML algorithm built a predictive, explanatory, mathematical model from the remotely retrieved, capture point,eco-georeferenced, LULC datasets and their seasonal, land cover in ArcGIS (i.e., "training data") in order to make robust predictions of unknown, foci. In so doing, the specificity introduced by the coexistence of spectral and spatial, eco-georeferenced, *Ae. aegypti*, artificial water, container, habitat, time series, empirical,RGB signatures in the drone library widened the swath, real time, information, UAV retrieval capacity.

Subsequently, we employed an Ordinary kriged-based stochastic, real time model in Spatial Analyst employing the capture point *Ae aegypti,* habitat RGB, signature, waveband ratios as the dependent variable in a regression-based matrix in the real time dashboard ArcGIS module.   Next, to fit the LULC, capture point, *Ae. aegypti* forecast model, signature estimators, we employed an exponential empirical semivariogram in Spatial Analyst. For each bin, the real time environment formulated the squared difference from the UAV geo sampled, eco-georeferenced, experimental plots and the real time, captured, RGB, frequency, count, discrete, integer values and then multiplied the signals by 0.5 to attain one empirical semivariogram signature value per bin in the real time dashboard. The binned orthomosics of the geosampled,LULC capture point's revealed local variation in the semivariogram/covariance RGB signature, endmember values. The drone database recorded the GPS location of the potential super-breeder site as a pin on a Google Earth image.

The real time, resampled habitat, RGB values were then analyzed by grouping (binning) the empirical, semivariogram/covariance, eco-georeferenced, LULC, capture points together employing square cells that were one lag wide. In the dashboard real time Geostatistical Analyst, the lag size and number of lags derived from the interpolated, RGB, *Ae. aegypti* capture point, signature ,wavelengths were iteratively adjusted to fit each prognosticated, eco-georeferenced, capture point. When the potential, hyperproductive, larval/pupal, capture point, habitat samples were located on a sampling grid, the grid spacing (1km x1km) revealed a good indicator of lag size in the dashboard. A rule of thumb is to multiply the lag size by the number of lags, which should be about half the largest distance among all sampled points (Cressie 1993). We noted that the range of the fitted, real time semivariogram, UAV, capture point, RGB, signature, frequency, LULC model, parameterized estimator,unmixed dataset for the Hillsborough County, epi-entomological, intervention, study site was very small relative to the extent of the *Ae. aegypti*, ,capture point, real time semivariograms. Conversely, if the range of the fitted semivariogram model is large relative to the extent of the empirical semivariogram, the lag size can be increased in ArcGIS (www. esri.com).

We employed the sub-meter resolution, RGB signature, UAV, seasonal, wavelength LULC, reflectance datasets for determining timing of immature, *Ae.aegypti*, mosquito immature productivity during the sample, capture point trials. The real time, geosampled, drone datasets were compared for optimal mapping of seasonal, mosquito, capture point, breeding site foci employing Fisher's exact test on two-by-three contingency tables (e.g., two habitat   capture point geolocations using three landscape categories) with, imaged, UAV grid cells representing sampled RGB signature values for each experimental plot, for each LULC category. All real time, drone exploratory, visual assessments were constructed in the UAV platform. Binomial sign tests, Fisher's tests, and linear regression were performed also in the platform.

To consider complications from spatial autocorrelation, coefficients we plotted second order autocorrelation statistics in the real time ArcGIS dashboard using an eigenvector spatial filtering function(ESF). The ESF employed a set of synthetic RGB proxy variables, which were extracted as orthogonal eigenvectors from a weighted spatial filter matrix that tied the habitats together in space and then adds these vectors as control variables to a RGB model specification. Here the real time UAV imaged spectral control variables identified and isolated the stochastic spatial dependencies among the eco-georeferenced, Ae aegypti, habitat,capture point, LULC observations, thus allowing model building to proceed as if the observations were independent. The real time ESF furnished a method to properly analyze an eco-georeferenced Ae .aegypti, geoclassified, real time, LULC,.capture point variable by effectively separating, spatially structured, random, RGB, signature components from trend and random noise present in

the variable. Positive spatial autocorrelation (i.e., like terms aggregating in geosapce) in a remotely sensed, seasonal, eco-georeferenceable, LULC, vector mosquito, forecast endmember model partly results from light reflectance scattering, rather than being neatly contained in pixel capture point boundaries, hence spilling over into nearby habitat pixels measured by an overhead sensor [Jacob et al. 2008]. Spatial autocorrelation has many interprets: a nuisance parameter, self-correlation, landscape map pattern, a diagnostic tool, a missing variable, surrogate, pseudo-replicated data variable, a spatial process mechanism, a spatial spillover, and the outcome of areal unit demarcation. (Griffith 2003). Interpreting spatial autocorrelation in an iteratively, quantitatively interpolated sub-meter resolution, RGB signature*,* larval/pupal, habitat, capture point, LULC, eco-georeferenced, grid-stratified, risk map can aid in determining seasonal, conspicuous trends, gradients, swaths or mosaics across an epi-entomological, intervention study site (Jacob et al. 2011).

Autocorrelation statistics were determined in the interpolated, real time, *Ae.aegypti* capture point, RGB signatures sampled from the LULC, eco-georeferenced, experimental plots in the UAV platform to determine clustering tendencies in the empirical, ento-epidemiological datasets. We considered a real time, UAV sensed, capture point, LULC, wavelength constant as a degenerate case (i.e., a constant with no variance) of perfect positive spatial autocorrelation: once the UAV sampled, interpolated, RGB value of the *Ae. aegypti* capture point constant was known at a single, eco-georeferenced, experimental epi-entomological, seasonal foci geolocation, it was known at all LULC geolocations within a real time, dashboard, ArcGIS interpolation algorithm. Next, we considered an eco-geographically sampled, real time, capture point, LULC variable that portrayed a north-south (or east-west) linear trend across a vulnerability, forecast, *Ae. aegypti* habitat, seasonal, UAV, capture point, LULC eigenvector map. This UAV, real time, sampled, *Ae. aegypti* ,LULC, parameter estimator dataset had a mean of zero, hence we assumed it may be geometrically orthogonal to and uncorrelated with the capture point, , wavelength constant. We also assumed that the north-south and east-west, oriented, linear trend, gridded, LULC, capture point, signature, also were orthogonal and uncorrelated. The UAV, real time, geosampled, LULC variable with mean zero whose RGB wavelength magnitudes formed a 3-dimensional symmetric mound (i.e., seasonal, hyperproductive, LULC,eco-georeferenced, capture point, *Ae. aegypti* larval/pupal, artificial water container, experimental habitat foci) in the center of a forecast vulnerability, real time map constituted other mutually orthogonal and uncorrelated, signature, LULC, capture point, UAV, gridded, map patterns. Consequently, these real time UAV sampled, wavelength variables displayed maximum levels of positive spatial autocorrelation which was describable as global clustering patterns in the U real time dashboard. Alternating sequences of prolific, *Ae. aegypti*, seasonal, larval/pupal, habitat, capture points with either an east-west or a north-south orientation portrayed moderate positive spatial autocorrelation, and constituted regional, LULC map patterns. Alternating sequences of smaller, less productive, *Ae aegypti* larval/pupal habitats with either an east-west or a north-south orientation portrayed weak positive spatial autocorrelation, and constituted local, real time, mappable, capture point, LULC patterns. This fragmentation continued through randomness (zero spatial autocorrelation) based on the capture point ,LULC arrangements of increasingly alternating habitat sampled values (i.e., single value mounds and basins) in the Hillsborough study site which subsequently portrayed increasing negative spatial autocorrelation (i.e., dissimilar aggregation of *Ae aegypti*, habitat, RGB attributes in geospace). Most substantive, capture point,LULC, habitat, RGB signature, wavelength variables have geographic distributions that can be described by linear combinations of some subset of mutually orthogonal and uncorrelated wavelength varying sized, vector arthropod, mound-basin (Jacob et al. 2015).

Leveraging our research team's expertise, the app interface and experiences was built employing the Unity game engine software (Kim et al. 2014) and Vuforia 6 SDK (Ibanez 2013). The resulting app was functional for both Apple and Android devices as necessary.

The app is geared towards, real time, monitoring and surveillance of seasonal, capture points, *Ae aegpti,* mosquito, habitats and their geographic locations for mapping, unknown, prolific foci in a stochastic iterative interpolator.The app can take eco-georeferenced, seasonal, UAV, real time, captured, RGB signature ,iteratively interpolated datasets and identify LULC properties where statistically significant clusters of *Ae aegypti*, superbreeder breeding site, habitats are throughout a county abatement, intervention stusy site The drone can record the capture point GPS location of a seasonal, mosquito habitat geolocation as a pin on a Google Earth street map in seconds. Then county-level, control personnel can visit the tagged properties and encouraged or enforce the treatment of the breeding site. The app provides the most optimal direction to the capture points by mapping out the routes for multiple geographic markers in real time. There is also a feature for control personal to complete a report and mark a geographic location in Hillsborough County as "Complete" or "Not Complete", to verify the signature captured was the *Ae aegypti* habitat breeding area as indicated by the real time, UAV platform. The platform has the ability to include comments and upload photos. Data maybe stored in an ArcGIS database (spectral library) for future analysis, and to determine if a repeated trend occurs at specific abatement study site.

The app is able to plot photos, as well as measure distances between mosquito habitats for determining pertinent statistics (e.g., real time, RGB signature covariates of prolific, seasonal, capture point, eco-georeferenced LULC sites). Control personnel are now able to download and open saved seasonal, *Ae aegypti,* habitat, and land cover maps. They are able to pan, zoom, and locate breeding sites in real time, on time series, forecast, signature maps using GPS, pin-points overlaid onto Google Earth ^{TM} data on their smart phones. The users may then export the created place marks (e.g., GPS pinpoints associated to an unknown, prolific, *Ae aegypti*, aquatic, habitat foci to eco-georeferenceable, capture point geolocation) to various formats and share the signature data with other County personnel and researchers in real time ,A real time iOS app can be interfaced with a differentially corrected GPS (DGPS) mobile device to provide spatial coordinates for all superbreeder *Ae. aegypti* , specified, sensor readings. The overhead method can allow the user (county mosquito control personnel) to specifc.capture point, *Ae. aegypti,* foci, GPS coordinates and the immature habitat signatures on any property based on the spectral reflection generated by the habitat signatures. The end result of the UAV platform is readily available unknown,eco-georeferenced, geolocations of seasonal, aquatic, vector, mosquito larval/pupal, capture point, habitat foci, on simulated web maps and exportable GeoTIFF drone, orthomosaic, 3D, topological, LULC sub-meter resolution, RGB sub-meter resolution signatures with various 3-D, products in a spectral library in a mobile, ArcGIS, real-time, dashboard module. These capture points can be demarcated with differentially corrected GPS coordinates (with a positional accuracy of 0.178m), in a deliminated text file.

3   SCENARIO PLANNING, EXPERIMENTAL FUTURING THROUGH PREDICTIVE ANALYTICS

Predictive analytics and computational models can provide public health officials with risk profiles, resource estimates and vulnerability assessments to support better mitigation, preparedness, response and recovery capabilities in the face of a natural disaster. As discussed, employing Real-Time UAV surveillance mapping to support identifying geolocations of vector-borne disease superbreeder sites, is one such tool. With the onset of these climate-related disasters and the possibility of mass migrations, scenario planning provides a well-established methodology to address such uncertainty about the future occurrence and impacts of climate-related events. With spatial-temporal analysis described that geo-locates superbreeder sites, the stage is set to integrate social disparity and vulnerability models, ecological perspectives and public policy to support an integrated vector management approach. As noted in Bardosh et al (2017:11), '…addressing VBDs into the future demands that we take a health systems approach, in terms of strengthening existing initiatives, the ability to translate knowledge into action and the capacity for organizations to promote community-based efforts'.

The dynamic complexity and uncertainties associated with climate change and extreme weather events, make scenario planning ripe for exploitation in exploring the public health implications of such natural disasters. Schwartz et al. (2019:133) describes scenarios '… as challenging descriptions of alternative future states (also referred to as "futures") that are relevant to a strategic decision and are representative of plausible developments in the external world'. Combining scenario planning and predictive analytics supports an experimental furturing framework that informs public health strategy development and strategic interventions. Extreme weather events can cause first order disasters and second order public health emergencies. Through predictive analytics described, vulnerability analysis (biophysical, social, spatial) can be assessed. Scenarios emerging from this can support across the disaster management domain (mitigation, preparedness, response and recovery). As such this takes experimental futuring to a new level of impact: in effect, linking future, predictive analytics with strategy.

It operationalizes plausibility-based scenarios characterized by increasing uncertainty and complexity and reframes the strategic discourse with real-time data. It is about proactive, forward looking, anticipatory futuring. The hazard of place model (Cutter, 1996) thereby becomes operational.

4   CONCLUSION

Climate change and the increase in the severity of extreme weather events and natural disasters has compromised public health conditions particularly in vulnerable communities thereby highlighting disparities across populations defined spatially. The complex spatial-temporal dynamics associated with climate related events, social, economic, political and environmental problem space influence the emergence and distribution of vector-borne diseases (VBDs) thereby shaping the public health landscape. As noted by Cutter et al. (2000:717), 'the social and biophysical vulnerability elements mutually relate and produce the overall vulnerability of the place'. Here we developed a customized, iOS application (app) for identifying geolocations

of superbreeder, Aedes aegypti, capture point, habitat properties in Hillsborough County from real time acquisitions of sub-meter resolution (e.g., 30 centimeter), land use land cover (LULC) images obtained from a drone unmanned aircraft. This real-time, predictive analytic capability changes the playfield with respect to scenario planning to support public health strategic intervention initiatives.

REFERENCES

Bardosh, K.L., Ryan, S.J., Ebi, K., Welburn,S., Singer,B. (2017) Addressing vulnerability, building resilience: community-based adaptation to vector-borne diseases in the context of global change. Infectious Diseases of Poverty (2017) 6:166

Berrang-Ford L, Harper SL, Eckhardt R. Vector-borne diseases: Reconciling the debate between climatic and social determinants. Can Comm Dis Rep 2016;42:211-2.

Cressie, N. (1993), Statistics for Spatial Data, rev. ed., Wiley.

Cutter,S.L., Mitchell, J.T., &. Scott,M.S. (2000) Revealing the Vulnerability of People and Places: A Case Study of Georgetown County, South Carolina, Annals of the Association of American Geographers, 90:4, 713-737.

Heyman et al (2015) Global health security: the wider lessons from the west African Ebola virus disease epidemic. Vol 385 May 9, 2015 www.thelancet.com

Jacob B, Novak RJ, Toe L, Sanfo MS, Cali Lampman RL skhan S, et al. (2013) Unbiasing a Stochastic Endmember Interpolator Using ENVI Object-Based Classifiers and Boolean Statistics for Forecasting Canopied Simulium damnosum s.l. Larval Habitats in Burkina Faso. J Geophys Remote Sensing 2(7): 6-73.

Jacob BG, Novak RJ (2016) Pernicious quasi-normal non-monotonic Poissionian non-negativity constraints for optimally rectifying incompatibilistic endeogeneity in sub-meter resolution pseudo-Euclidean regression space employing analogs of the Pythagorean theorem and parallelogram laws for semi-parametrically demarcating non-trivial land cover wavelength filters and time series impulse-response metrological functions in an invertible Hermitian transjugate matrix while consolidating synergistic semi-logarithmic non- ordinate axis-scaled covariances in C++ for forecasting episodical yellow fever sylvatic, case distributions in an eco-geo referenceable irrigated riceland complex in Gulu, Uganda Journal of Applied Mathematics and Statistics 3(4): 42-366.

Jacob BG, Shafer S, Alinda P, Loun D, Mc Kinnon A, et al. (2017) Lexicographically, cartesian-ordered, differential calculi in canonically extractable in-situ near infra-red fluorescence quantum spectroscopic sub-surface continuous geodesic fluxions for metaheuristic chlorophyll- a translucent emissivty mapping intermittently canopied immature narrow riverine tributary Simulism damnosum sl oviposition sites for bio-optically delineating multivariate normalized Gaussian processes elucidative administrated by prior covariances and a spline within a reproducing non-frequentist simultaneous diagonalization of amalgamized positive definite kernels in Hilbert space: Implementation of a 'Slash and Clear' control intervention in two eco-georeferenceable agro-village complexes in northern Uganda Uganda Journal of Geophysics and Remote sensing 4(5): 26-221.

Jacob BG, Novak RJ (2014) Integrating a Trimble Recon X 400 MHz Intel PXA255 Xscale CPU®Mobile Field Data Collection System Using Differentially Corrected Global Positioning System Technology and a Real Time Bidirectional Actionable Platform within an ArcGIS Cyberenvironment for Implementing Mosquito Control. Advances in Remote Sensing 3(3): 141-196.

Jacob BG, Morris JA, Caamano EX, Griffith DA, Novak RJ (2011) Geomapping generalized eigenvalue frequency distributions for predicting prolific Aedes albopictus and Culex quinquefasciatus habitats based on spatiotemporal field-sampled count data Acta Tropica 2: 61-68.

Jacob BG, Novak RJ, Toe LD, Sanfo M, Griffith DA, Lakwo TL, et al. (2013) Validation of a Remote Sensing Model to Identify *Simulium damnosum* s.l. Breeding Sites in Sub-Saharan Africa. *PLoS Neglected Tropical Diseases* 7(7): 32-42.

Jacob BG. Mwangangi JM Mbogo CB, Novak RJ (2011) A Taxonomy of Unmixing Algorithms Using Li- StrahlerGeometric- Optical Model and other Spectral Endmember Extraction Techniques for Decomposing a QuickBirdVisible and Near Infra-red Pixel of an *Anopheles arabiensis* Habitat *Open Remote Sensing* 17(3)-11-24.

Lee, B., Preston, F., Green, G. (2012) Preparing for High-impact, Low-probability Events: Lessons from Eyjafjallajökull. Chatham House Report, January 2012.

Reina Ortiz, R., Le, N.K., Sharma, V., , Hoare, I., Quizhpe, E., Teran, E., Naik, E., Salihu,H.M., Izurieta, (2017) Post-earthquake Zika virus surge: Disaster and public health threat amid climatic conduciveness.

Schwarz, J.O., Ram, C., Rohrbeck, R., (2019) Combining scenario planning and business wargaming to better

anticipate future competitive dynamics. Futures, Volume 105, January 2019, Pages 133-142

Sheehan,M.C.,Fox,M.A., Kaye,C., and Resnick,B. (2017) Integrating Health into Local Climate Response: Lessons from the U.S. CDC Climate-Ready States and Cities Initiative. Environmental Health Perspectives. Available at: https://ehp.niehs.nih.gov/doi/pdf/10.1289/EHP1838